Hindawi
Geofluids
Volume 2022, Article ID 3341741, 9 pages
https://doi.org/10.1155/2022/3341741

Research Article

Coupled Analysis of Thermofluid-Structure Field for Thermal Properties of Early-Age Concrete Influenced by Electric Heating System

Lin Liu,[1] Yue Zhao,[2] Jianyong Han,[3,4] Cheng Cheng,[5] and Chaozhe Zhang[6]

[1]*School of Civil Engineering, Shenyang Jianzhu University, Shenyang, Liaoning 110000, China*
[2]*Science and Technology Service Platform, Qilu University of Technology (Shandong Academy of Sciences), Jinan, Shandong 250000, China*
[3]*School of Civil Engineering, Shandong Jianzhu University, Jinan, Shandong 250101, China*
[4]*Key Laboratory of Building Structural Retrofitting and Underground Space Engineering (Shandong Jianzhu University), Ministry of Education, Jinan, Shandong 250101, China*
[5]*School of Mechanics and Civil Engineering; State Key Laboratory for Geomechanics and Deep Underground Engineering, China University of Mining and Technology, Xuzhou, Jiangsu 221116, China*
[6]*School of Transportation, Southeast University, Nanjing, Jiangsu 211189, China*

Correspondence should be addressed to Yue Zhao; zhaoy@sdas.org and Jianyong Han; hanlwb@163.com

Received 1 August 2022; Revised 28 September 2022; Accepted 1 October 2022; Published 19 November 2022

Academic Editor: Yi Xue

Copyright © 2022 Lin Liu et al. This is an open access article distributed under the Creative Commons Attribution License, which permits unrestricted use, distribution, and reproduction in any medium, provided the original work is properly cited.

When heat energy is transferred to concrete through energy conversion by an electric heating system, the overall thermal performance of the early-age concrete is affected by the local high temperature of the concrete. This, in turn, affects the accuracy of the prediction and calculation of concrete deformation. Concrete thermal physical parameter models considering the mutual influence of heat and humidity were established to clarify the influence of an electric heat tracing system on the heat transfer performance of concrete at an early age, based on the concepts of equivalent age and hydration degree. Additionally, the COMSOL numerical simulation software was used for realizing the numerical solution of concrete heat transfer. The research indicates that the degree of hydration is affected by the heating provided by the electric heat tracing system. When curing for 40 h, the degree of hydration approaches 0.82 and remains unchanged, which indicates that the hydration of cement was almost complete in less than 2 days. The specific heat value of concrete in the early stage was significantly affected by electric heat tracing. This value of concrete at a high initial temperature was larger than that at a low temperature, while the specific heat of each point in the later stage tended to be the same. The thermal conductivity was significantly affected by the local electrical heating. The higher the temperature was, the lower the thermal conductivity was, which remained stable for two days under the influence of temperature. The key contribution of this research is to provide a coupling model for concrete curing. The findings from the study also provide industry practitioners with a comprehensive guide regarding the specific applications of the electric heating system in early-age concrete curing.

1. Introduction

Currently, concrete is the most commonly used building material, of which deformation and cracks are affected by the construction method [1–4]. As a winter concrete heating and curing method, the local high temperature provided by the electric heating system influences the overall structural performance of the concrete, which results in obvious cracks on the surface after the concrete is hardened [5–7]. Thus far, the thermal and mechanical parameters of concrete in the later stage of hardening are basically used to calculate the deformation of concrete during the curing period; however, the thermal and mechanical parameters of concrete in the early stage are evidently different from those in the later

stage of hardening [8]. If the changes of thermal and mechanical parameters generated by the concrete material during the hydration process are not considered, the calculation results of the temperature field and deformation will be affected. Moreover, the current test procedures for the thermal and mechanical properties of concrete are all measured under standard temperature and humidity conditions. However, the actual temperature and humidity of concrete at an early age vary greatly, and the temperature and humidity interact with the hydration process of concrete [9–11]. Therefore, when studying the influence of an electric heating system on concrete performance, it is necessary to consider factors such as the local high temperature caused by the electric heating cable, asynchronous hydration process, temperature, and humidity to improve the accuracy of the concrete heat transfer calculation, concrete deformation, and crack resistance.

Currently, based on the concept of equivalent age and degree of hydration, researchers have focused on the deformation of concrete by temperature and humidity. These efforts mainly consider the influence of temperature and humidity on the mechanical and thermal properties of concrete and on the mathematical model for optimizing mechanical and thermal parameters and deformation [12, 13]. Zhong et al. [14, 15] successively conducted concrete shrinkage, swelling, internal temperature, and moisture tests and proposed a theoretical calculation model of the relationship between concrete temperature, internal moisture, and strain. Pane and Hansen [16] proposed a method for calculating the early stress development of concrete through experiments regarding creep, heat, autogenous deformation, early stress development, hydration kinetics, and early stress prediction. They proved that stress prediction accuracy can be increased based on the hydration heat, relaxation modulus, autogenous shrinkage, and temperature history. Huang et al. [17] investigated the action law and mechanical behavior of key parameters of wetting force regarding the healing process based on the coupling model of the wetting force. Based on the coupling effect of chemical-heat-mechanical-moisture, Chen et al. [18–20] successively analyzed the influence of concrete deformation, pouring time process, environmental temperature, moisture, steel bar, etc. on the stress and deformation of concrete. The quantitative relationship between the stress degeneration and the concrete hydration degree, temperature, and moisture is established, and the multifield coupling deformation and crack model of concrete was proposed. Considering the influence of hydration heat on temperature and stress based on the thermal-mechanical coupling model, Zhao et al. and Hu et al. [21, 22] conducted research on concrete temperature control. Zheng and Wei [23] conducted 2D and 3D mesoscale model investigations with polygon and polyhedral aggregates and established a chemothermal coupling model of concrete.

The above studies have well proven that the thermal and mechanical parameters of concrete based on the hydration process can predict the temperature and deformation development more accurately. However, these thermal and mechanical parameters do not fully consider the temperature, moisture, and hydration processes simultaneously.

Therefore, using the heat conduction model and solid mechanics model in the COMSOL numerical analysis software, this study considers the influence of temperature and moisture, establishes concrete thermal and mechanical parameter models based on the hydration degree, and conducts temperature field simulation analysis. The above studies have proven that the thermal and mechanical parameters of concrete considering the hydration process are more conducive to accurately predicting the development of temperature and deformation. However, when studying the thermal parameters, temperature, humidity, and hydration process are not completely considered simultaneously. Therefore, based on the concept of the hydration degree, a concrete thermal parameter model considering the influence of temperature and humidity was established in this study, and COMSOL numerical analysis software was used to study the variations of thermal parameters and temperature field.

2. Concrete Thermophysical Parameters Based on the Hydration Degree

2.1. Equivalent Age. The two concepts of equivalent age and maturity reflect the same problem. Regarding this problem, at the earliest time, Nurse [24] and Saul [25] proposed the concept of concrete maturity based on steam curing experiments, which proved that maturity and concrete strength were equivalent, and established the "Nurse-Saul" maturity equation.

$$M = \sum_{0}^{t} [T(t) - T_0)]\Delta t, \tag{1}$$

where M is the maturity coefficient; t is the curing age, h; T is the temperature at age t, ˚C; and T_0 is the initial temperature, ˚C, which takes the value -10˚C.

Subsequently, according to the concept of maturity, the concrete age at different curing temperatures can be transformed into the equivalent age at the same maturity:

$$t_e = \frac{\sum (T - T_0)\Delta t}{T_r - T_0}, \tag{2}$$

where t_e is the equivalent age and T_r is the reference concrete temperature, ˚C, which is generally 20˚C under standard curing condition.

Hansen and Pedersen [26] carried out hydration heat experiments under different curing temperatures and proposed an equivalent age mathematical model based on the Arrhenius function as follows:

$$t_e = \sum_{0}^{t} \exp\left[\frac{E_a}{R}\left(\frac{1}{273 + T_r} - \frac{1}{273 + T_c}\right)\right]\Delta t, \tag{3}$$

where T_c is the curing temperature, ˚C, and E_a is the concrete activation energy, J/mol. When T_c is greater than or equal to 20˚C, $E_a = 33.5$; when T_c is less than 20˚C, $E_a = 33.5 + 1.47(20 - T_c)$.

2.2. Hydration Degree. The hydration degree reflects the concrete hydration degree at a certain age, which is significantly affected by the water-cement ratio, mineral admixtures, cement fineness, and curing temperature [27]. Mills [28] and Hansen [29] found that the hydration reaction stops before the cement is completely reacted and consumed, which means that the concrete hydration degree does not reach the value of 1. Lin and Meyer [30] proposed a final hydration formula based on cement fineness and curing temperature as follows:

$$\alpha_u = \alpha_{u293} \exp\left[-0.00003(T-293)^2 \cdot SGN(T-293)\right],$$
$$\alpha_{u293} = \frac{\beta_1 \times (w/c)}{\beta_2 + (w/c)} \le 1.0, \tag{4}$$

where α_{u293} is the final cement hydration degree at a curing temperature of 20°C (293 K), α_u is the final hydration degree considering the curing temperature, and β_1 and β_2 are based on the specific surface area function.

2.3. Specific Heat Capacity. The specific heat capacity of water is 4.18 kJ/(kg·°C), which is greater than the specific heat capacity of concrete materials. Therefore, the moisture content has a certain influence on the specific heat capacity of the material. As the moisture content increases, the specific heat capacity also increases. Low et al. [31] propose the relationship between the concrete specific heat capacity and moisture content.

$$c_w = c_d + \xi_c \times \omega, \tag{5}$$

where c_w is the specific heat capacity of wet concrete, kJ/(kg·°C); c_d is the specific heat of dry concrete, kJ/(kg·°C); ξ_c is the increase in specific heat capacity for every 1% increase in moisture content, kJ/(kg·°C), which may take a value of 0.028 kJ/(kg·°C); and ω is the concrete moisture content.

Van [32] proposed a concrete specific heat formula that considers the mixing ratio, specific heat capacity, hydration degree, and current concrete temperature, which states that

$$c = \frac{W_c \alpha c_{cef} + W_c(1-\alpha)c_c + W_a c_a + W_w c_w}{\rho},$$
$$c_{cef} = 0.0084T_d + 0.339, \tag{6}$$

where c is the specific heat capacity when the degree of hydration is α, kJ/(kg·°C); W_c, W_a, and W_w are the weight of cement, aggregate, and water in each cube, respectively, kg/m^3; c_c, c_a, and c_w are the specific heat capacities of cement, aggregate, and water, respectively, kJ/(kg·°C); c_{cef} is the assumed specific heat capacity of cement paste, kJ/(kg·°C); ρ is the concrete density, kg/m^3; α is the hydration degree; and T_d is the current temperature.

Accordingly, a formula for estimating the specific heat of concrete during the curing period was proposed:

$$c[(\alpha(t_e), \omega)] = c + 0.028\omega, \tag{7}$$

where $c[(\alpha(t_e), \omega)]$ is the specific heat capacity when the degree of hydration is α and water content is w, kJ/(kg·°C).

2.4. Thermal Conductivity Coefficient. Based on Schindler's formula and Low's results [31], a formula for calculating the thermal conductivity coefficient of concrete was established considering the influence of the concrete moisture content and hydration degree:

$$\lambda[(\alpha(t_e), \omega)] = \lambda_u(1.33 - 0.33a) + \zeta_\omega \omega, \tag{8}$$

where $\lambda[(\alpha(t_e), \omega)]$ is the thermal conductivity when the degree of hydration is α and water content is w, kJ/(m·h·°C), and λ_u is the final thermal conductivity coefficient, kJ/(m·h·°C), which should be experimentally determined.

In this study, the thermal conductivity value of a 28-day dry test block was adopted. ζ_w is the increase in the thermal conductivity when the moisture content increases by 1%.

2.5. Humidity Parameters

2.5.1. Cement Hydration and Self-Drying. Cement hydration consumes water, which reduces concrete humidity. Zhang et al. [33] proposed a mathematical model for predicting the decrease in concrete humidity caused by the water consumption of cement hydration through the concrete humidity test.

$$H_d = \begin{cases} 0, & \alpha \ge \alpha_h, \\ (1 - H_{d,u})\left(\dfrac{\alpha - \alpha_h}{\alpha_u - \alpha_h}\right)^{\beta_H}, & \alpha < \alpha_h, \end{cases} \tag{9}$$

where H_d *is the humidity reduction caused by cement hydration*, %; $H_{d,u}$ is the relative humidity at the end of hydration; and α_h and β_H are empirical coefficients.

2.5.2. Moisture Diffusion. The diffusion of humidity is affected by the temperature difference, humidity difference, water-cement ratio, and other factors. Gong [34] proposed a moisture diffusion coefficient for early-age concrete based on the equivalent age concept considering the influence of temperature on hydration degree.

$$\frac{D(t_e)}{t_e \cdot D_{sat}} = \alpha_0 + \frac{1 - \alpha_0}{1 + ((1-H)/(1-H_c))^n}, \tag{10}$$

where $D(t_e)$ is the humidity diffusion coefficient based on the concept of equivalent age, considering the effect of temperature; D_{sat} is the humidity diffusion coefficient when saturated; and α_0, H_c, and n are empirical coefficients.

3. Governing Equation

3.1. Heat Conduction Equation. The concrete hydration reaction is related to its own temperature, moisture, age, etc., and its thermal conductivity also changes continuously with the hydration reaction. Therefore, the heat release and heat conduction in concrete hydration involves a complex nonlinear problem. According to the literature, a heat

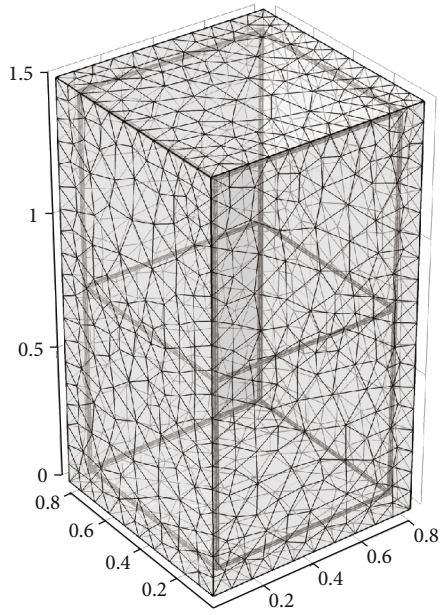

Figure 1: Numerical model grid diagram.

transfer equation can be established based on the hydration degree considering moisture change.

$$\rho c[(\alpha(t_e),\omega)]\frac{\partial T}{\partial t} = \nabla\{\lambda[(\alpha(t_e),\omega)]\nabla T\} + \frac{\partial Q_{\alpha(t_e)}}{\partial t}, \quad (11)$$

where considering the effect of temperature, based on the effect of equivalent age, $Q_{\alpha(t_e)}$ is the cement hydration heat, kJ/kg.

3.2. Moisture Diffusion Model. Assuming that the form of moisture transfer in concrete is diffusion, the temperature gradient is the driving force behind moisture diffusion. Moreover, the self-drying in concrete hydration at an early age will cause decreased moisture content. Accordingly, the moisture diffusion equation is

$$\frac{\partial H}{\partial t} = \nabla(D(t_e)\nabla H) - \frac{\partial H_d}{\partial t}. \quad (12)$$

4. Multiphysics Coupling Simulation Calculation Using COMSOL

Based on the heat and moisture physical parameters and transfer equations of temperature and moisture changes, numerical simulation of the early-age concrete temperature field is performed using the multiphysics coupling numerical analysis software COMSOL Multiphysics, as illustrated in Figure 1, with dimensions of 0.8 m × 0.8 m × 1.5 m in length × width × height. Each key parameter is calibrated referring to the temperature field test data of the concrete test column embedded with a heating belt. Tables 1 and 2 list the symbols for the heat and moisture transfer parameters required by the model. Figure 2 illustrates the heating belt and layout of the measuring points. The black line in the figure represents the heating belt, and the black dots represent the measuring points.

Table 1: Symbols required for heat transfer simulations.

Symbols	Symbol value	Symbols	Symbol value
ρ (kg/m^3)	2500	T_r (°C)	20
E_a (J/mol)	33500	R (J/(mol·K))	8.314
α_u	0.82	W_w (kg)	200
W_c (kg)	400	W_a (kg)	1661
λ_μ (kJ/(m·h·K))	7.185	c_c (kJ/(kg·K))	1.14
c_a (kJ/(kg·K))	0.678	c_w (kJ/(kg·K))	4.187

Table 2: Symbols required for moisture transfer simulations.

Symbols	Symbol value	Symbols	Symbol value
α_{u293}	0.8	α_u	0.8
α_c	0.72	$H_{s.u}$	0.83
β_H	3	a_o	0.05
H_c	0.8	n	15
R (J/(mol·K))	8.314	T_r (K)	293

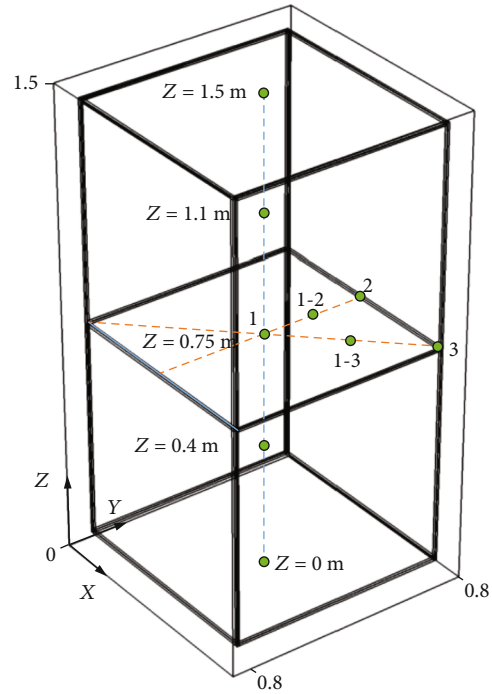

Figure 2: Schematic of temperature layout monitoring point.

The initial temperature condition of the concrete specimen is the concrete entering mold temperature T_0 288 K (e.g., 15°C). The boundary conditions of the model were set as two kinds of surface contact conditions of the test specimen, including the external surface of test column, and the contact surface between concrete and electric heating belt. To simulate the thermal insulation measures taken in the test, the surface of the test column was wrapped with

Table 3: Equivalent exothermic coefficients of concrete specimen surface.

Boundary location	Equivalent heat release coefficient (kJ/(m^2·h·K))	Calculation time (h)	
		0-72	72-200
Outer surface of test column	β_{t1}	8.3	
Contact surface between concrete and tracer	β_{t2}	418.6	0

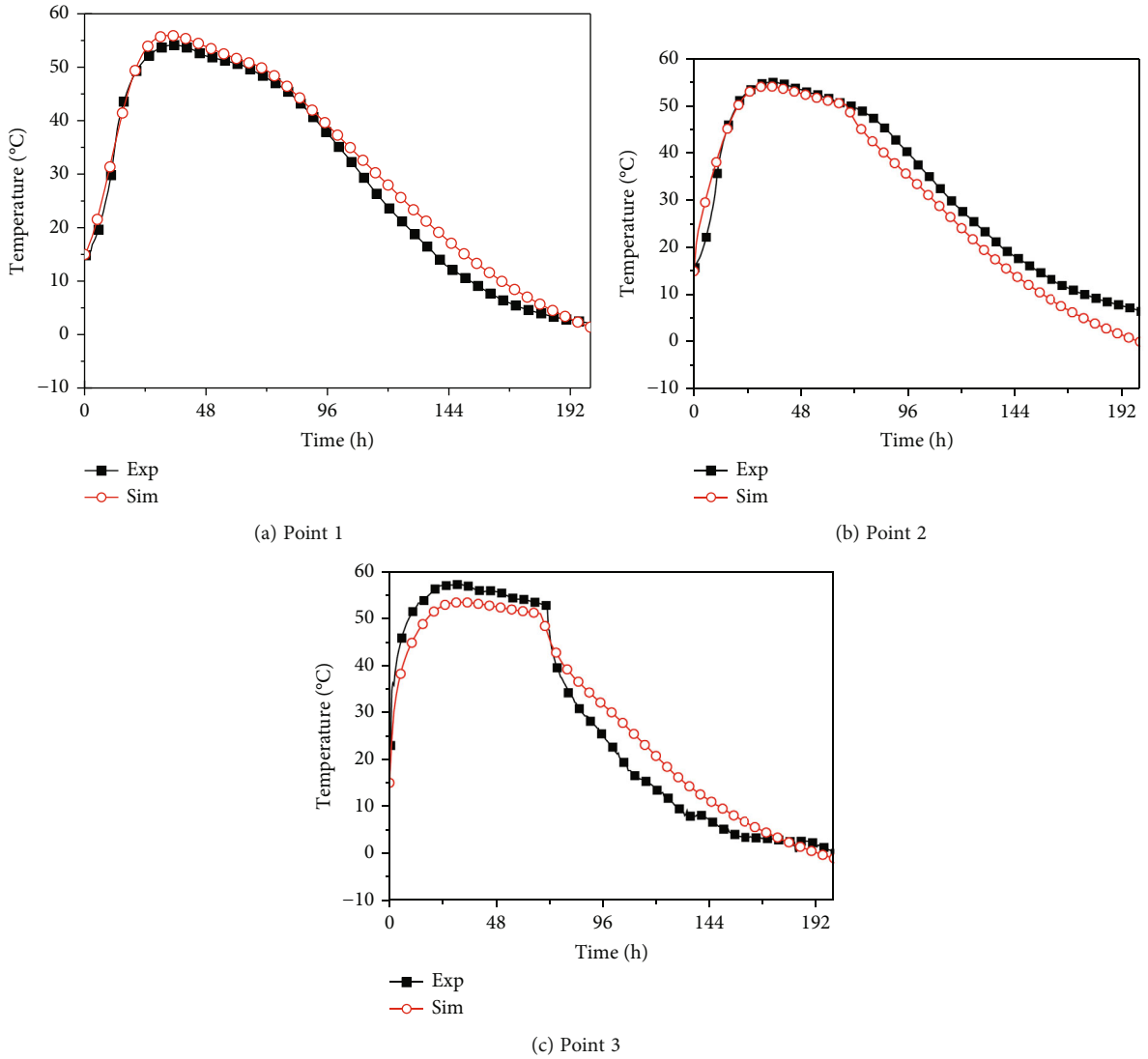

Figure 3: Curves for the comparison test value and the calculated value.

a thermal insulation layer. The boundary conditions on the outer surface of the test specimen were realized by selecting the equivalent heat release coefficient β_t, which is regarded as the third type of boundary conditions. The contact surface between concrete and the electric heating belt is the fourth type of boundary condition. Table 3 illustrates equivalent exothermic coefficients of the concrete specimen surface.

4.1. Model Validity Verification. The numerical calculation results are compared with the experimental data, and the numerical model is calibrated. Figure 3 depicts a comparison between the test column temperature data and numerical calculation results. The established calculation model had a higher degree of coincidence with the measured data, and the variations were approximately the same. Slight deviations exist in the comparison curves when in the late curing time. The main reason for the deviation between the calculation results of the model and measured results is the heat transfer coefficient of the insulation layer of the test specimen and the accuracy of the equivalent thermal conductivity of the concrete. The nonuniform density caused by the installation of the insulation layer of the specimen will have a certain effect on the results of the temperature field. However, the uniform equivalent heat transfer coefficient was

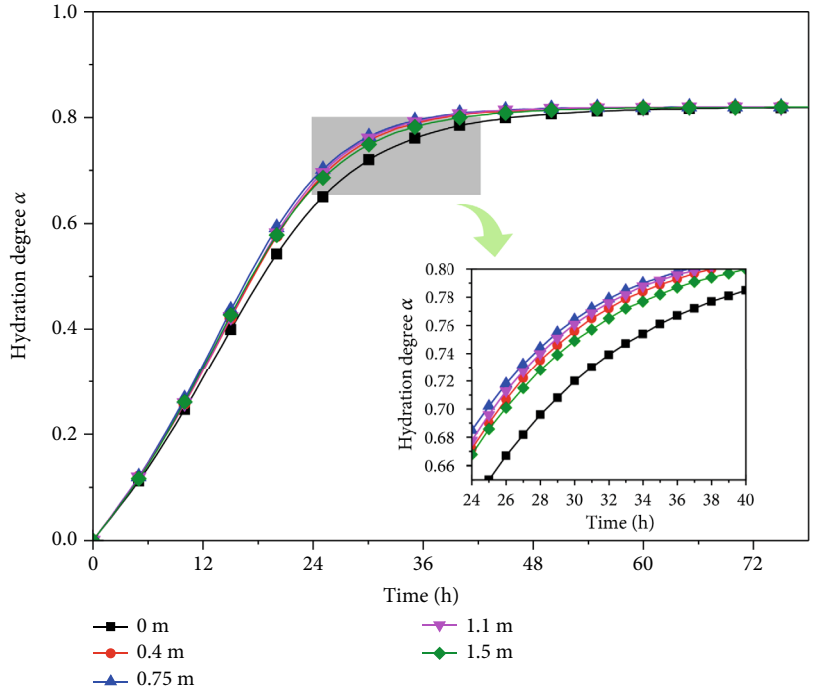

Figure 4: The degree of hydration at different heights with time under the influence of temperature.

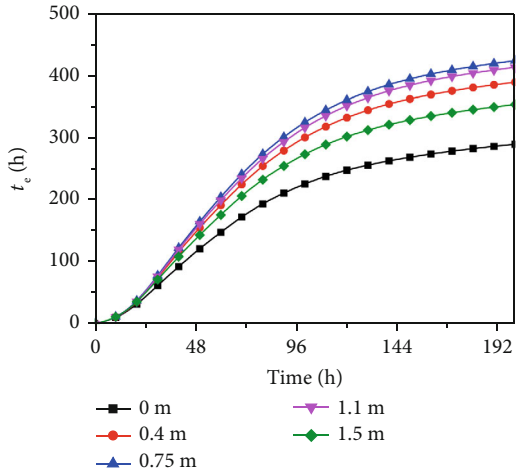

Figure 5: The equivalent age at different heights with time under the influence of temperature.

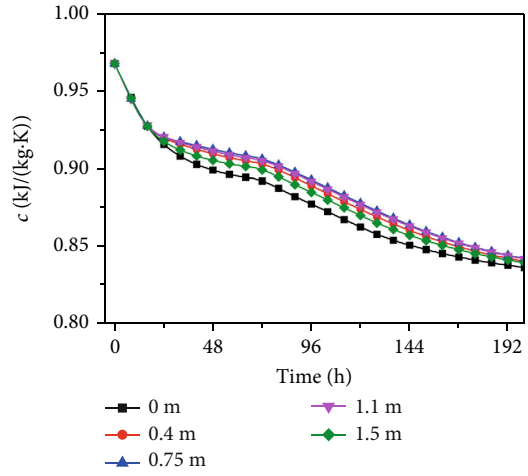

Figure 6: The specific heat value at different heights changes with time under the influence of temperature.

adopted in the numerical model to simplify the model establishment, which did not consider the nonuniform effect caused by the installation. In addition, as a heterogeneous and anisotropic material, the thermal conductivity of concrete is not completely consistent. A unique thermal conductivity was used in the numerical model. Based on the comparisons, the accuracy of the numerical model for predicting the multiphysical coupling behavior was verified.

4.2. Variation of Thermophysical Parameters. To explore the variation of the key parameters of the temperature field model, the built-in 3D intercept function in the COMSOL software was used to determine the thermal parameters at different heights of the model vertical center with age. The variation of hydration degree of the concrete column at different vertical heights over time is shown in Figure 4. Although the hydration degrees at different heights are relatively close at the same time, it still presents the distribution characteristics that the high-temperature area in the middle has a higher hydration degree than the low temperature area at both ends. When t is equal to 40 h, the hydration degree gradually approaches 0.82, which proves that the hydration reaction is basically completed in less than 28 days.

The different hydration degrees at different positions of the concrete column are due to the different temperatures measured at each point. The equivalent ages of the concrete at different heights were analyzed, as shown in Figure 5. Affected by the embedded heat source, the concrete equivalent

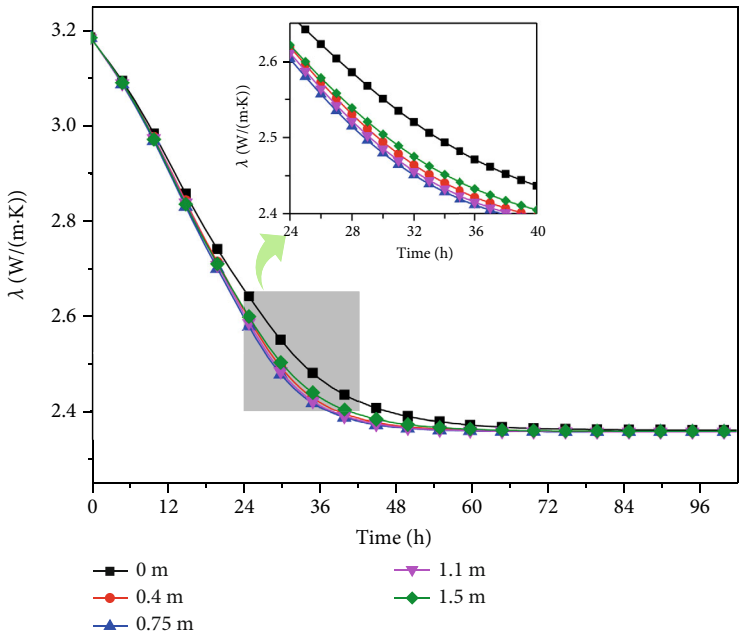

Figure 7: Thermal conductivity at different heights changes with time under the influence of temperature.

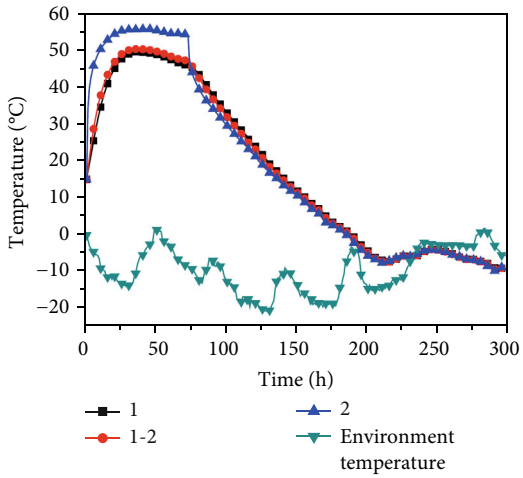

Figure 8: Temperature change from center to edge.

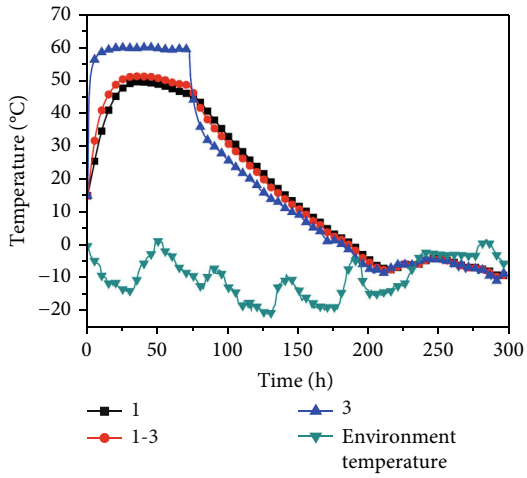

Figure 9: Temperature change from center to corner.

age was much higher than the actual curing time. For instance, under a curing time of 200 h, the equivalent age of each point of the concrete column was approximately 250 h ~400 h, which is 1 to 2 times that of the curing time. Therefore, during the electric heating process of the concrete column, hydration reaction proceeded rapidly, and the model conformed to the actual hydration reaction conditions.

With the continuous change of the temperature distribution inside the concrete column and continuous progress of the cement hydration reaction, the thermal parameters measured at different positions in the concrete column also change constantly.

The curve describing the change of the specific heat of the concrete column at different heights over time is shown in Figure 6. When the concrete is poured into the mold, the specific heat value of the concrete is approximately 0.9678 kJ/(kg·K). Owing to the continuous progress of the concrete hydration reaction, the specific heat value decreased nonlinearly and gradually stabilized. Within 20 h after pouring, the specific heat values of each point were not significantly different. The specific heat value of concrete is significantly affected by the concrete temperature and hydration degree. After 30 h of pouring, due to the different temperature gradients and hydration degrees inside the concrete, the specific heat values at each point were significantly different. The specific heat value at the bottom of the concrete column was the lowest, while the highest specific heat value appeared in the upper part of the concrete. If it is cured for 200 h after pouring, the specific heat value of each point inside the concrete column structure is not significantly different with an average of 0.836 kJ/(kg·K), which is approximately 86% of the initial specific heat value.

Figure 7 illustrates the relationship curve describing the change in the thermal conductivity coefficient at different vertical heights of the concrete columns with curing time. In the figure, the change in the thermal conductivity is roughly inversely proportional to the degree of hydration; i.e., the thermal conductivity coefficient decreases with the development of concrete hydration. Compared to the specific heat value, the thermal conductivity coefficient decreases faster and tends to be stable for approximately 50 h. The initial value of the thermal conductivity coefficient was 3.185 W/(m·K), while the final thermal conductivity coefficient of concrete was 2.36 W/(m·K), which is approximately 74% of the initial value.

4.3. The Variation of Temperature Field. According to the analysis of the intermediate data surface of the test specimen, as shown in Figures 8 and 9, the entire temperature process can be divided into the rapid temperature rise stage, temperature stable stage, and rapid temperature cooling stage.

Rapid temperature rise stage: the temperature of the three monitoring points increased rapidly owing to the influence of the heating belt.

Relatively stable stage: as the concrete hydration exothermic temperature reaches a stable level, affected by the heat transfer of the heating belt, the corner temperature is the highest and the edge temperature is the lowest. The temperature gradient at each point was very close during the slow decline in the temperature.

Rapid temperature cooling stage: the temperature at the monitoring points begins to drop continuously as the heating belt stops the power supply; the temperature gradient at the corner points is the highest. When the heating belt is out of power, the temperature curve has an obvious inflection point. This is consistent with the experimental data in terms of the temperature process and temperature changes.

5. Conclusion

Concrete hydration heat release and heat conduction involve complex nonlinear issues. Based on the concept of equivalent age hydration degree, this study considers the influence of the hydration degree and moisture and revises the mathematical model of thermal conductivity and specific heat capacity. This provides an important research basis and method for the study of key thermal parameters of early-age concrete and improves the accuracy of the simulation study of the concrete temperature field, which lays a theoretical and technical foundation for optimizing the heating and curing design method and construction measures and innovating the curing and engineering application of concrete in winter. Our research takes an embedded concrete test column with a heating belt as an example to simulate and calculate the thermophysical parameters. The following conclusions are drawn:

(1) Curing temperature affects the hydration degree of equivalent age. The hydration reaction of the concrete column occurred rapidly during the heating process. The model proposed in this study was verified according to the actual hydration reaction. When the curing time reached 40 h, the hydration degree gradually approached 0.82 and remained unchanged. The hydration reaction was basically completed within 28 d

(2) The specific heat of concrete is significantly affected by the concrete temperature and hydration degree. The greater is the initial temperature, the greater the specific heat, and the value tends to be consistent in the later stage

(3) The thermal conductivity coefficient changed approximately opposite to the hydration degree. With the development of concrete hydration degree, the thermal conductivity gradually decreases

(4) The multiphysical coupling model proposed in this study guarantees the accuracy prediction of the mechanical behaviors of early-age concrete. This is a beneficial attempt for the coupled analysis of early-age concrete, which is an important guideline for the curing treatment for the early-age concrete in winter

However, the scope of this research is relatively limited. To further improve the research accuracy and applicability, complex condition experiments will be conducted in the future, and more accurate numerical simulations will be performed by comparing and optimizing equations.

Data Availability

Some or all data, models, or code that support the findings of this study are available from the corresponding author upon reasonable request.

Conflicts of Interest

The authors declare that they have no conflicts of interest.

Acknowledgments

This work was supported by the Doctoral Research Fund of Shandong Jianzhu University (Grant X19080Z).

References

[1] Y. Xue, J. Liu, X. Liang, S. Wang, and Z. Ma, "Ecological risk assessment of soil and water loss by thermal enhanced methane recovery: numerical study using two-phase flow simulation," *Journal of Cleaner Production*, vol. 334, article 130183, 2022.

[2] J. Wang, J. Han, J. Chen et al., "Experimental and numerical study on the dynamic response of a superthick backfill subgrade under high-speed railway loading: a case study of Qianjiang-Zhangjiajie-Changde railway," *Journal of Construction Engineering and Management*, vol. 148, no. 12, 2022.

[3] P. Hou, Y. Xue, F. Gao, S. Wang, X. Jiao, and C. Zhu, "Numerical evaluation on stress and permeability evolution of overlying coal seams for gas drainage and gas disaster elimination in

protective layer mining," *Mining Metallurgy & Exploration*, vol. 39, no. 3, pp. 1027–1043, 2022.

[4] J. Shi, B. Liu, F. Zhou et al., "Heat damage of concrete surfaces under steam curing and improvement measures," *Construction and Building Materials*, vol. 252, article 119104, 2020.

[5] J. Liu, Y. Xue, Q. Zhang, H. Wang, and S. Wang, "Coupled thermo-hydro-mechanical modelling for geothermal doublet system with 3D fractal fracture," *Applied Thermal Engineering*, vol. 200, article 117716, 2022.

[6] W. Li, Z. Huang, G. Hu, W. H. Duan, and S. P. Shah, "Early-age shrinkage development of ultra-high-performance concrete under heat curing treatment," *Construction and Building Materials*, vol. 131, pp. 767–774, 2017.

[7] T. Shi, C. Deng, J. Zhao, P. Ding, and Z. Fan, "Temperature field of concrete cured in winter conditions using thermal control measures," *Advances in Materials Science and Engineering*, vol. 2022, Article ID 7255601, 12 pages, 2022.

[8] X. Zeng, C. Ma, G. Long, H. Dang, and Y. Xie, "Hydration kinetics of cement composites with different admixtures at low temperatures," *Construction and Building Materials*, vol. 225, pp. 223–233, 2019.

[9] J. Han, D. Liu, Y. Guan et al., "Study on shear behavior and damage constitutive model of tendon-grout interface," *Construction and Building Materials*, vol. 320, article 126223, 2022.

[10] Z. Mi, Y. Hu, Q. Li, X. Gao, and T. Yin, "Maturity model for fracture properties of concrete considering coupling effect of curing temperature and humidity," *Construction and Building Materials*, vol. 196, pp. 1–13, 2019.

[11] W. Long, J. Wei, Y. Gu, and F. Xing, "Research on dynamic mechanical properties of alkali activated slag concrete under temperature-loads coupling effects," *Construction and Building Materials*, vol. 154, pp. 687–696, 2017.

[12] B. Cho, D. Park, J. Kim, and H. Hamasaki, "Study on the heat-moisture transfer in concrete under real environment," *Construction and Building Materials*, vol. 132, pp. 124–129, 2017.

[13] Y. Tian, N. Jin, and X. Jin, "Coupling effect of temperature and relative humidity diffusion in concrete under ambient conditions," *Construction and Building Materials*, vol. 159, pp. 673–689, 2018.

[14] Z. Zhong, L. P. Huang, and H. Zhang, "Research on humidity field and self-restraint stress field in concrete," *Bulletin of the Chinese Ceramic Society*, vol. 40, no. 8, pp. 2609–2621, 2021.

[15] S. Li, Y. Yang, Q. Pu, W. Wen, and A. Yan, "Thermo-hydro-mechanical combined effect analysis model for early-age concrete bridges and its application," *Advances in Civil Engineering*, vol. 2020, Article ID 8864109, 15 pages, 2020.

[16] I. Pane and W. Hansen, "Predictions and verifications of early-age stress development in hydrating blended cement concrete," *Cement and Concrete Research*, vol. 38, no. 11, pp. 1315–1324, 2008.

[17] K. Huang, B. Wu, K. Tang, and Z. Li, "Hygro-chemical-mechanical multi-field coupling analysis on damage-healing behavior of concrete," *Chinese Quarterly of Mechanics*, vol. 42, no. 3, pp. 490–497, 2021.

[18] H. Chen, G. Deng, and Y. Q. Zhang, "Simulation of faced rock-fill dams considering temperature change and long-time deformation," *Journal of Hydroelectric Engineering*, vol. 40, no. 10, pp. 124–134, 2021.

[19] W. T. Huang and F. Y. Gong, "Numerical simulation of creep behavior for RC beam through a hydro-thermo-mechanical approach," *Low Temperature Architecture Technology*, vol. 43, no. 5, pp. 86–90, 2021.

[20] J. Y. Wu, W. X. Chen, and Y. L. Huang, "Computational modeling of shrinkage induced creaking in early-age concrete based on the unified phase-field theory," *Chinese Journal of Theoretical and Applied Mechanics*, vol. 53, no. 5, pp. 1367–1382, 2021.

[21] Z. Zhao, Y. Zhong, X. Li, and Y. Sun, "Tensile creep of dam concrete at early age under variable temperature history," *Journal of Hydroelectric Engineering*, vol. 39, no. 8, pp. 46–54, 2020.

[22] C. B. Hu, Z. H. Sun, and L. J. Wang, "Experimental study on the early-age stress behavior of cement concrete pavement," *Engineering Mechanics*, vol. 38, no. 6, pp. 163–174, 2021.

[23] Z. Zheng and X. Wei, "Mesoscopic models and numerical simulations of the temperature field and hydration degree in early-age concrete," *Construction and Building Materials*, vol. 266, article 121001, 2021.

[24] R. W. Nurse, "Steam curing of concrete," *Magazine of Concrete Research*, vol. 1, no. 2, pp. 79–88, 1951.

[25] A. G. A. Saul, "Principles underlying the steam curing of concrete at atmospheric pressure," *Magazine of Concrete Research*, vol. 2, no. 6, pp. 127–140, 1951.

[26] P. F. Hansen and E. J. Pedersen, "Maturity computer for controlling curing and hardening of concrete," *Nordisk Betong*, vol. 19, no. 1, pp. 21–25, 1977.

[27] H. Zhao, X. M. Wu, B. Gao, and G. G. Liu, "Influence of cement fineness on the deteriorate behavior of concrete," *Journal of Building Materials*, vol. 13, no. 4, pp. 520–523, 2010.

[28] R. H. Mills, "Factors influencing cessation of hydration in water cured cement pastes," *Highway Research Board Special Report*, vol. 90, pp. 406–424, 1966.

[29] T. C. Hansen, "Physical structure of hardened cement paste: a classical approach," *Materials and Structures*, vol. 19, no. 6, pp. 423–436, 1986.

[30] F. Lin and C. Meyer, "Hydration kinetics modeling of Portland cement considering the effects of curing temperature and applied pressure," *Cement and Concrete Research*, vol. 39, no. 4, pp. 255–265, 2009.

[31] K. S. Low, S. C. Ng, and N. H. Tioh, "Thermal conductivity of soil-based aerated lightweight concrete," *KSCE Journal of Civil Engineering*, vol. 18, no. 1, pp. 220–225, 2014.

[32] B. K. Van, "Simulation of hydration and formation of structure in hardening cement based material," *Computers and Structures*, vol. 80, pp. 2035–2204, 2002.

[33] J. Zhang, D. W. Hou, and Y. Gao, "Calculation of shrinkage stress in early-age concrete pavements. I: calculation of shrinkage strain," *Journal of Transportation Engineering*, vol. 139, no. 10, pp. 961–970, 2013.

[34] L. L. Gong, *Research on performance of self-compacting concrete and time dependent multi-field coupling analysis of concrete, [Ph.D. thesis]*, Zhejiang University, 2010.